Electronic Supplementary Information

Copper(II) Metal-Organic Framework with 2,2-Dimethylglutarate and Imidazole Ligands: Synthesis, Characterization and catalytic performance for cycloaddition of CO_2 to epoxides

Pelin Köse Yaman[a,b*], Sevde Demir[a], Serpil Denizaltı[c], Hakan Erer[a] and Okan Zafer Yeşilel[a]

[a]Dokuz Eylül University, Faculty of Science, Department of Chemistry, 35390, Izmir, Turkiye

[b]Eskişehir Osmangazi University, Faculty of Science, Department of Chemistry, 26040, Eskişehir, Turkiye

[c]Ege University, Faculty of Science, Department of Chemistry, 35100, Izmir, Turkiye

*Corresponding author. Fax: +90 2324534188.

E-mail address: pelin.kose@deu.edu.tr (P. Köse Yaman).

Table of contents

Section 1. Additional Structural Analysis

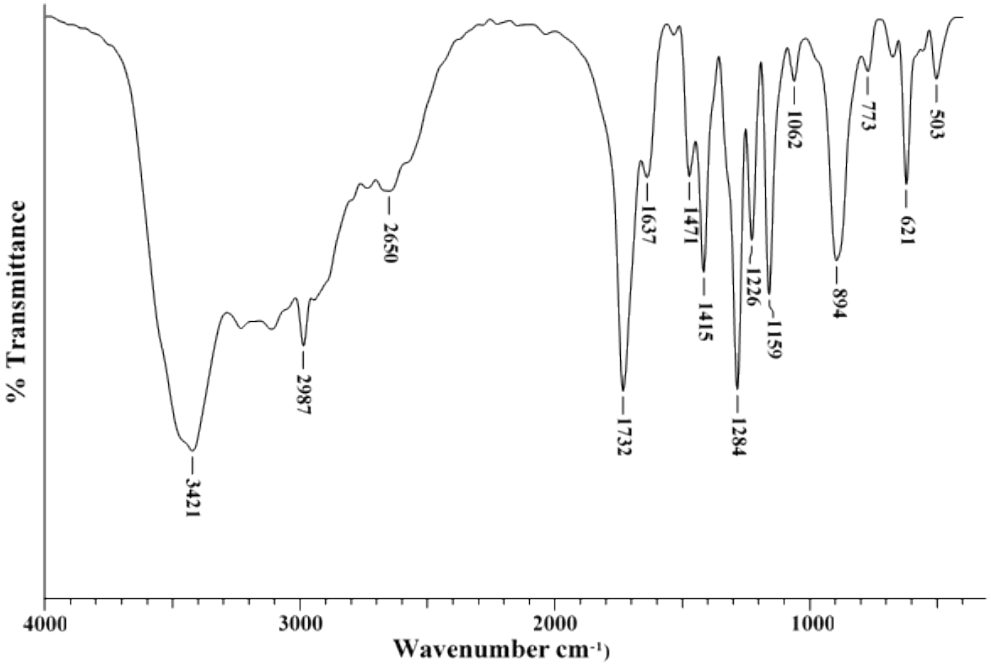

Fig. S1. FTIR spectrum of 2,2-dimethylglutaric acid ($dmgH_2$)

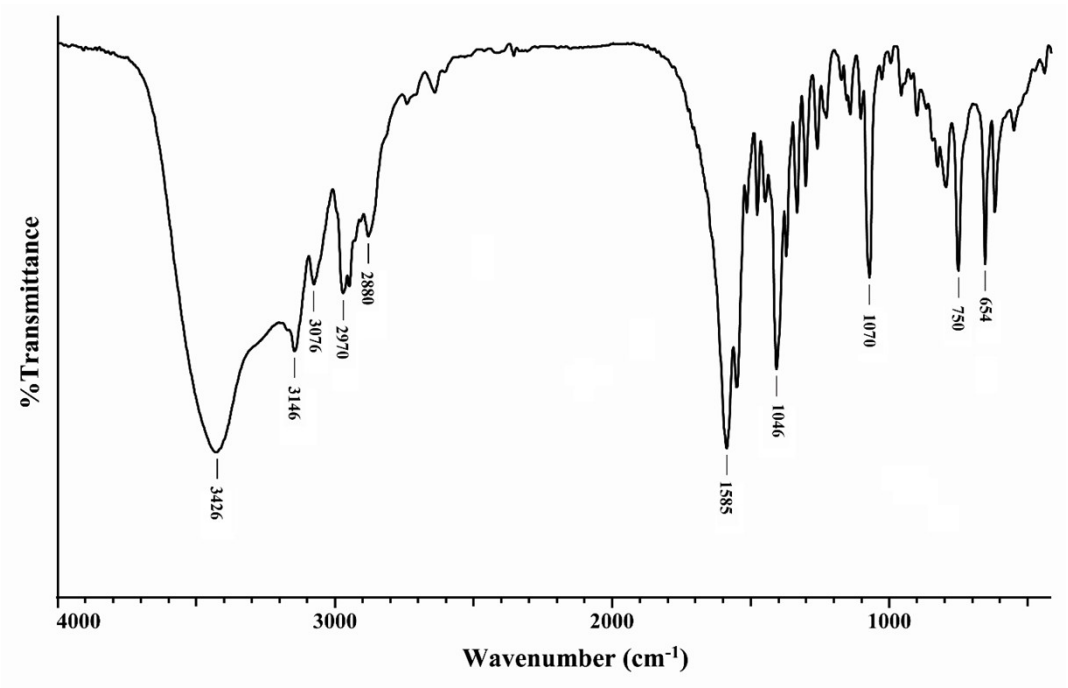

Fig. S2. FT-IR Spectrum of **1**

Section 2. Powder X-ray Diffraction (PXRD) Patterns

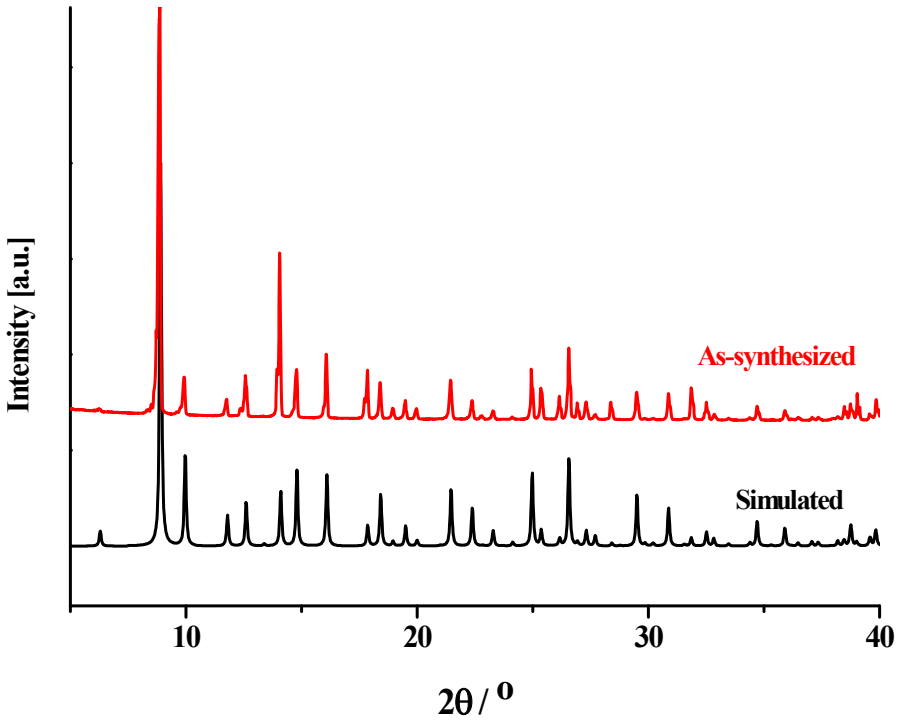

Fig. S3. Experimetal and calculated PXRD patterns of **1**

Section 3. Thermal analysis and Optical Absorption Results

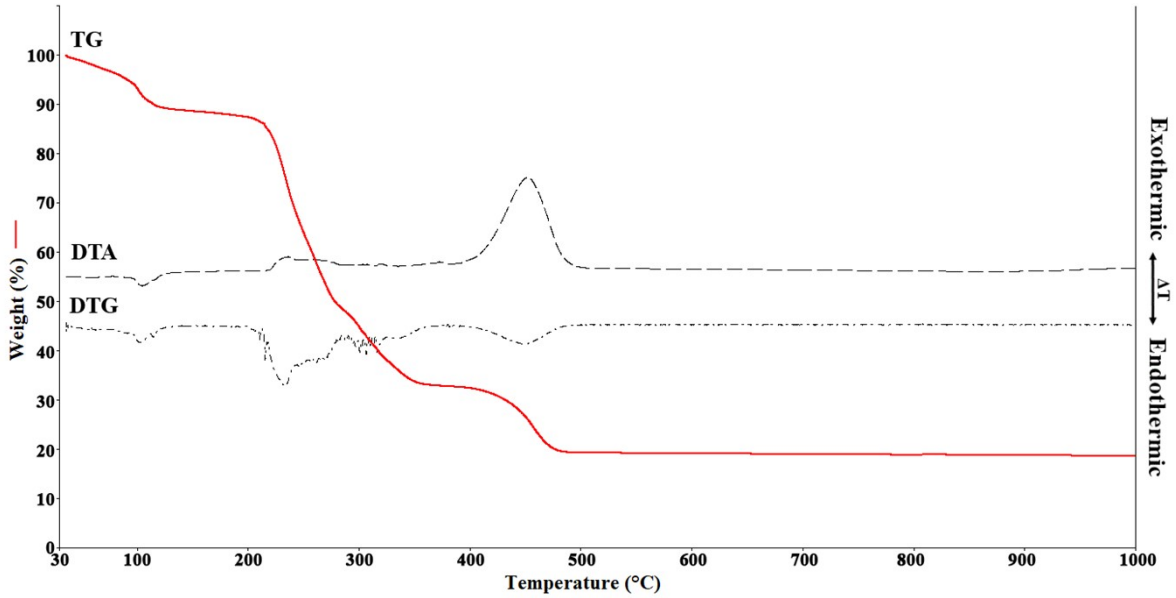

Fig. S4. The thermal analysis curves (TG, DTG and DTA) of **1**

Thermal properties of **1** were determined by simultaneous TG/DTA analysis (Fig. S4). The compound **1** shows a two-stage decomposition process. In the first step, **1** started to lose crystal water molecule in the range of 48–138 °C with an experimental mass loss of 12 % (calc. 13 %). The second stage of the temperature range of 189–506 °C for **1** is related to the decomposition of im and dmg ligands by exothermic effect ($DTA_{max.}$ = 452 °C). The final product of thermal decomposition was also identified as a CuO by IR spectroscopy (exp.:19.25, calc.:19.17%).

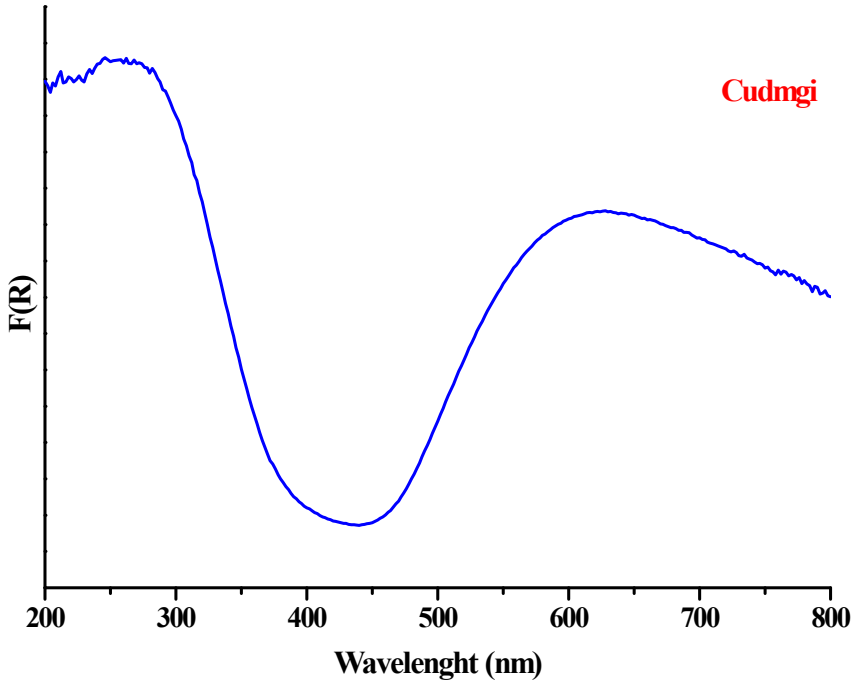

Fig. S5. UV-Vis spectra of **1**

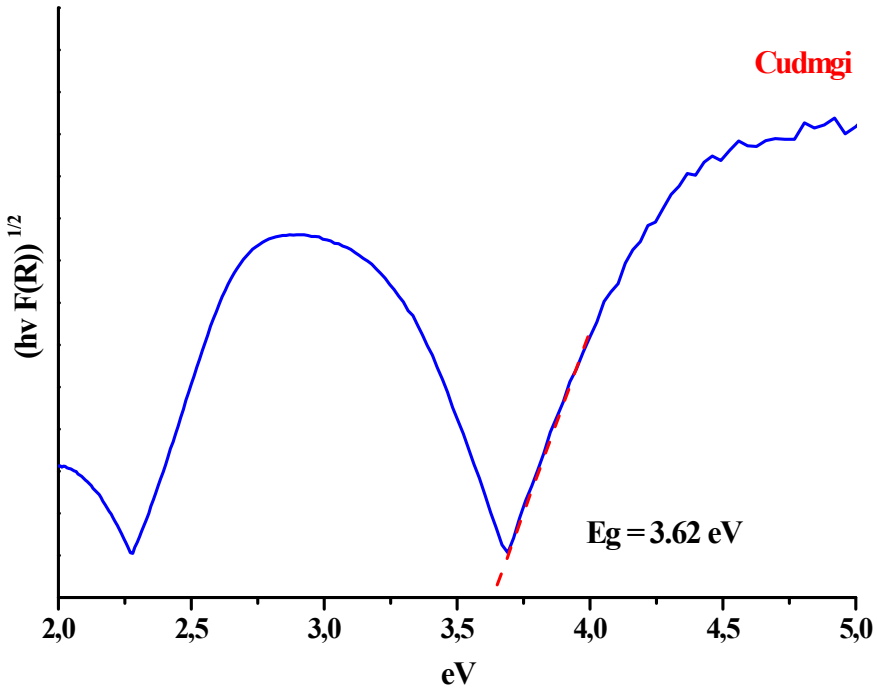

Fig. S6. The Kubelka-Munk plot as a function of energy for **1**

The optical band gaps (Eg) and semiconductor properties of **1** were investigated using solid state diffuse reflection spectrum at room temperature ($BaSO_4$ was used as reference material for measurements). Because of the data obtained, the calculated optical band gap (Eg) value of the complex and the Kubelka-Munk curves were plotted as a function of energy (Fig. S5). The equation [$(F(R) = (1-R)^2/2R)$], known as the Kubelka-Munk function, was used to determine the optical band gap value. By converting the data obtained from the reflection spectrum into absorption data, the photon energy versus $hV(F(R))^{1/2}$ [F(R); Kubelka–Munk function] curve was drawn and by extrapolating from the linear part of this curve, the optical band gap value of the complex was found (Eg= 3.62 eV). According to these results, the complex shows semi-conductor properties (optical band gaps of structures Eg= <4 eV show semiconductor properties) [1,2].

Section 4. Additional Crystallographic Parameters

Table S1. Selected bond distances and angles for **1** (Å, º)

Complex 1			
Cu1–O1	2.002 (3)	Cu1–N3	1.973 (3)
Cu1–O3^{i}	2.020 (3)	Cu1–N1	1.983 (3)
O1–Cu1–O3^{i}	177.12 (11)	N3–Cu1–N1	175.38 (14)
N3–Cu1–O1	92.21 (12)	N1–Cu1–O1	92.06 (13)
N3–Cu1–O3^{i}	88.47 (12)	N1–Cu1–O3^{i}	87.35 (13)

Symmetry codes: (i) $-y+5/4, x-1/4, z-1/4$; (ii) $y+1/4, -x+5/4, z+1/4$; (iii) $y+1/4, -x+3/4, -z+3/4$; (iv) $-y+5/4, x-1/4, z+3/4$; (v) $-y+1/2, -x+3/2, -z+3/2$.

Table S2. Hydrogen-bond geometry (Å, °) for **1**

D–H···A	**D–H**	**H···A**	**D···A**	**D–H···A**
N4–H4···O4^{iii}	0.86	1.92	2.765 (4)	167
N2–H2···O5^{iv}	0.86	2.17	2.909 (7)	144
O5–H5E···O2	0.85	2.01	2.662 (7)	133
O7–H7A···O6	0.85	1.99	2.792 (10)	157
O7–H7B···O7^{ii}	0.85	2.14	2.919 (6)	153
O6–H6D···O4	0.85	2.04	2.789 (6)	147
O6–H6E···O5	0.85	2.10	2.870 (10)	150

Symmetry codes: (ii) $y+1/4, -x+5/4, z+1/4$; (iii) $y+1/4, -x+3/4, -z+3/4$; (iv) $-y+5/4, x-1/4, z+3/4$.

Section 4. ^{1}H NMR Data From The Catalytic Reaction Results

(Table 2, Entry 1)

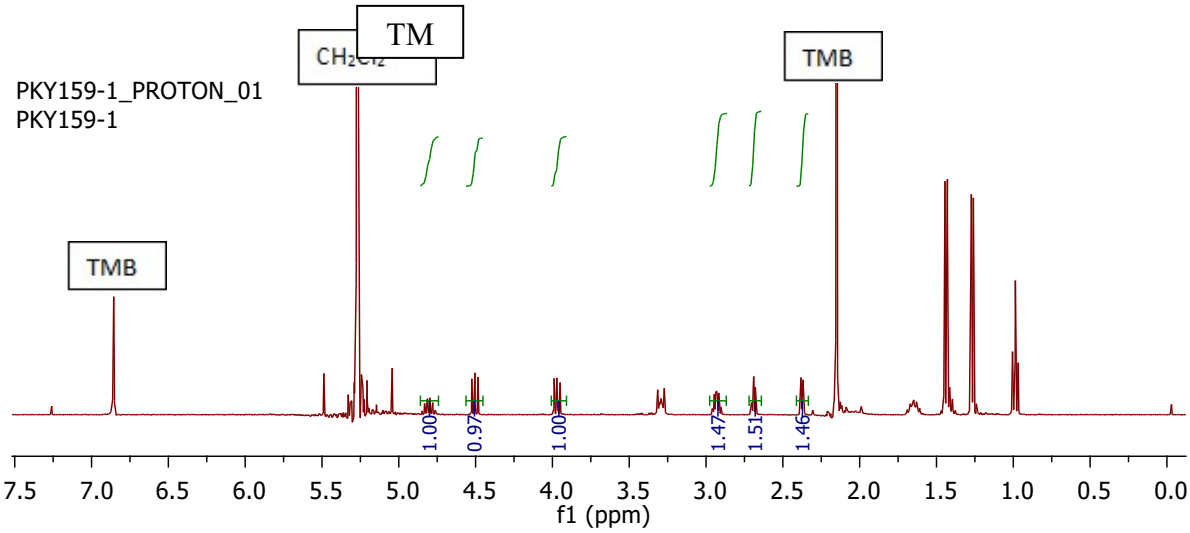

Fig. S7. The Catalytic Reaction Result of Entry 1

(Table 2, Entry 4)

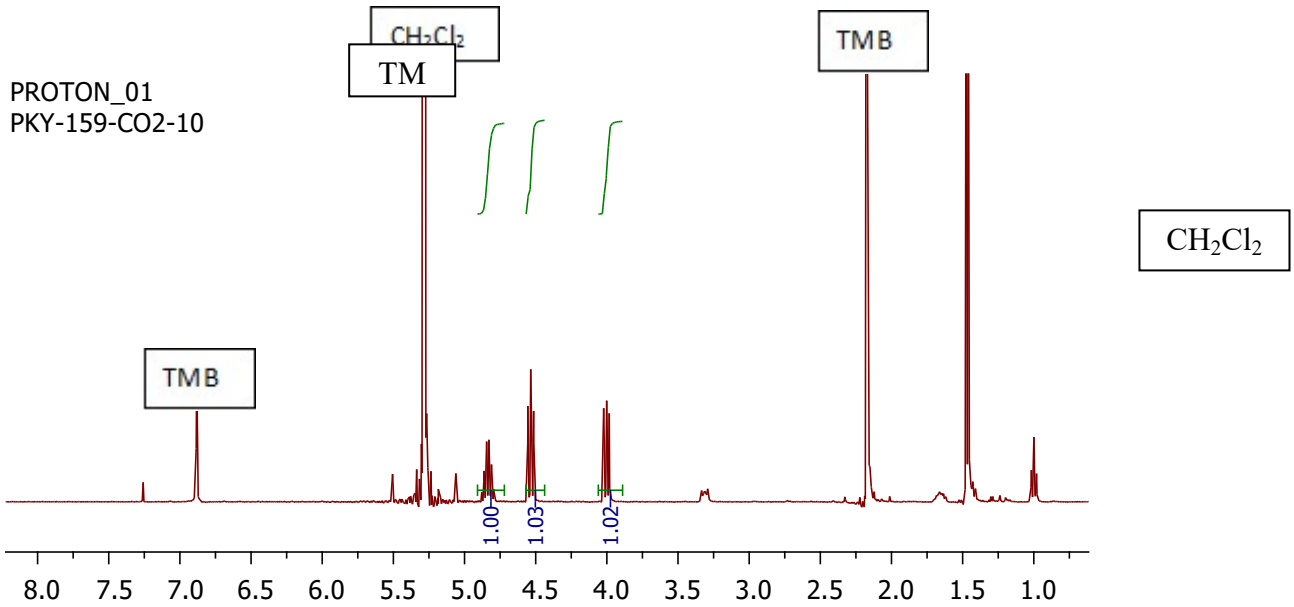

Fig. S8. The Catalytic Reaction Result of Entry 4

(Table 2, Entry 5)

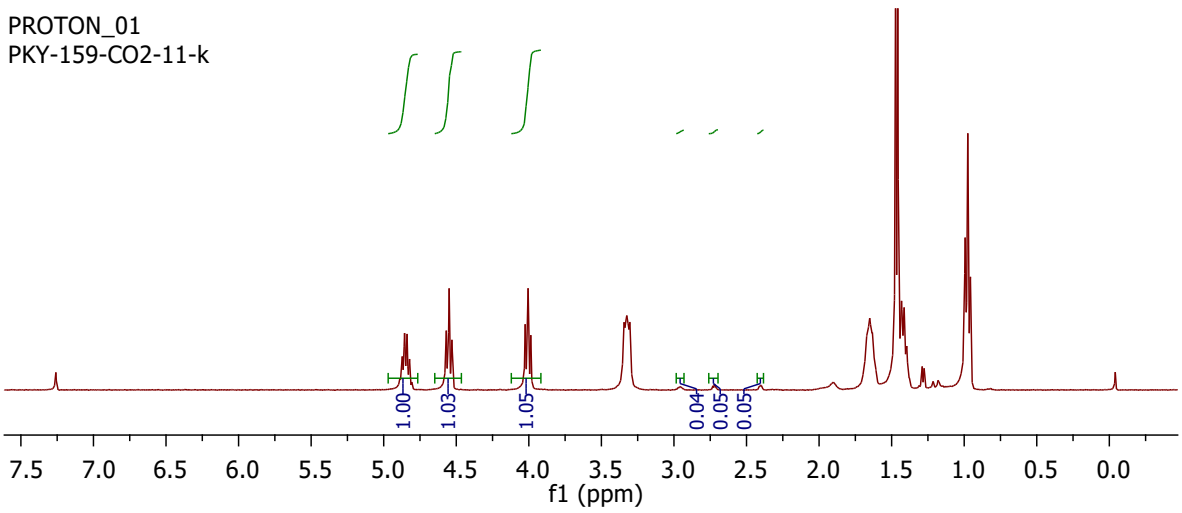

Fig. S9. The Catalytic Reaction Result of Entry 5

(Table 2, Entry 6)

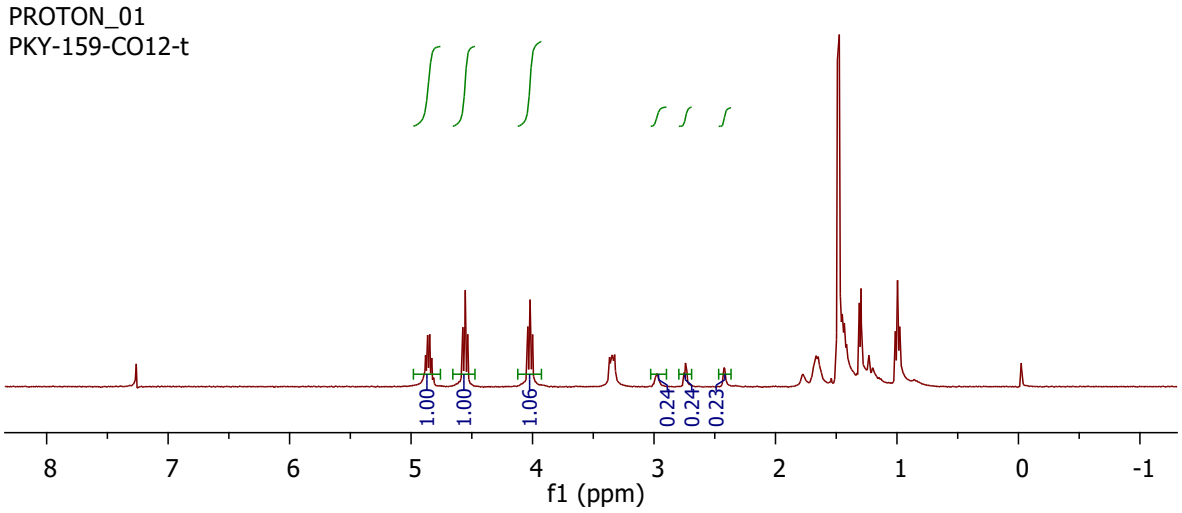

Fig. S10. The Catalytic Reaction Result of Entry 6

(Table 2, Entry 9)

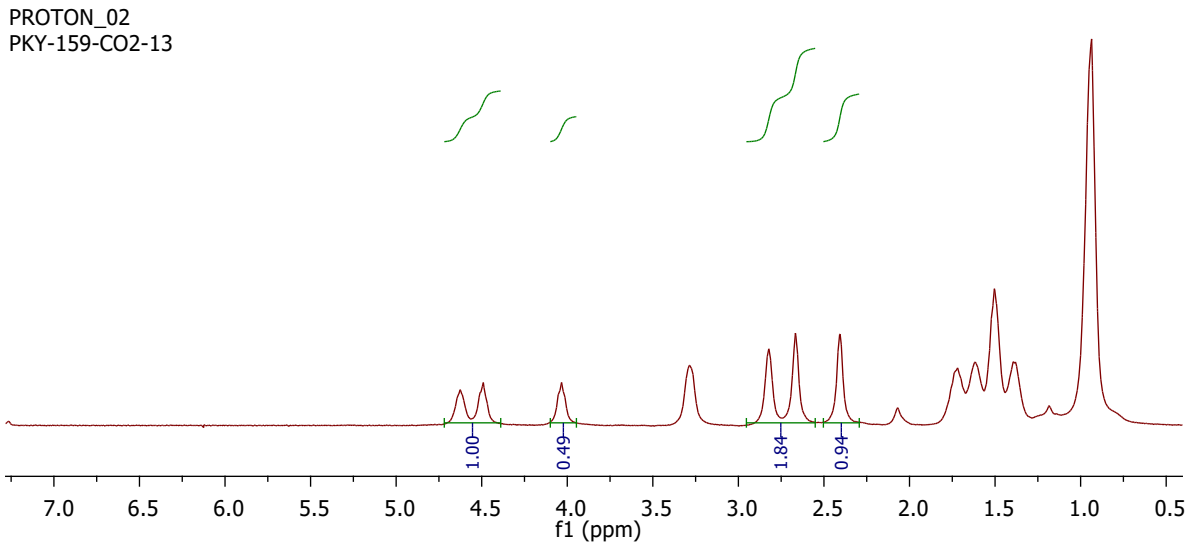

Fig. S11. The Catalytic Reaction Result of Entry 9

(Table 2, Entry 10)

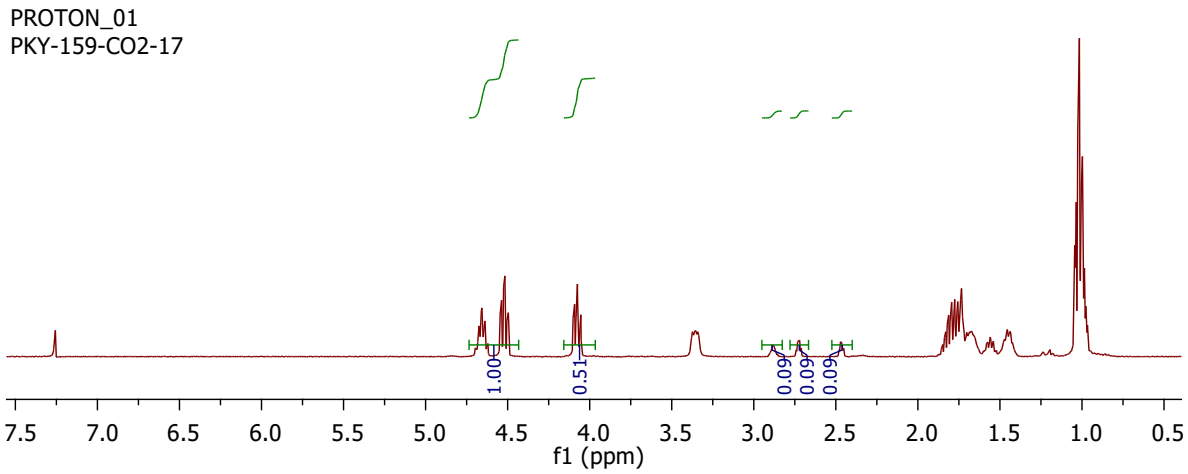

Fig. S12. The Catalytic Reaction Result of Entry 10

(Table 2, Entry 11)

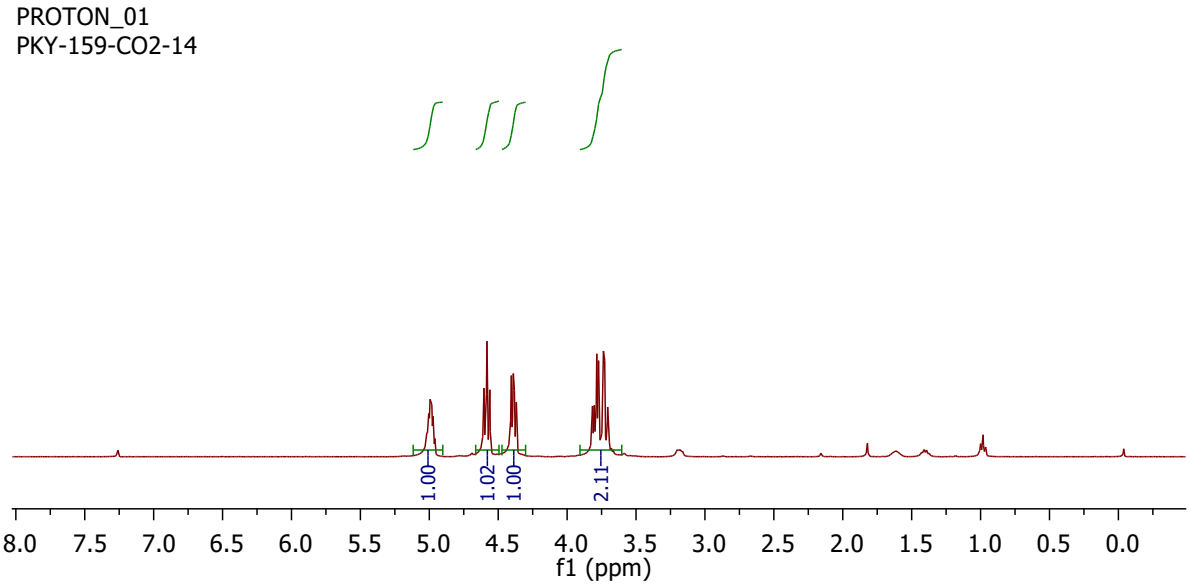

Fig. S13. The Catalytic Reaction Result of Entry 11

(Table 2, Entry 12)

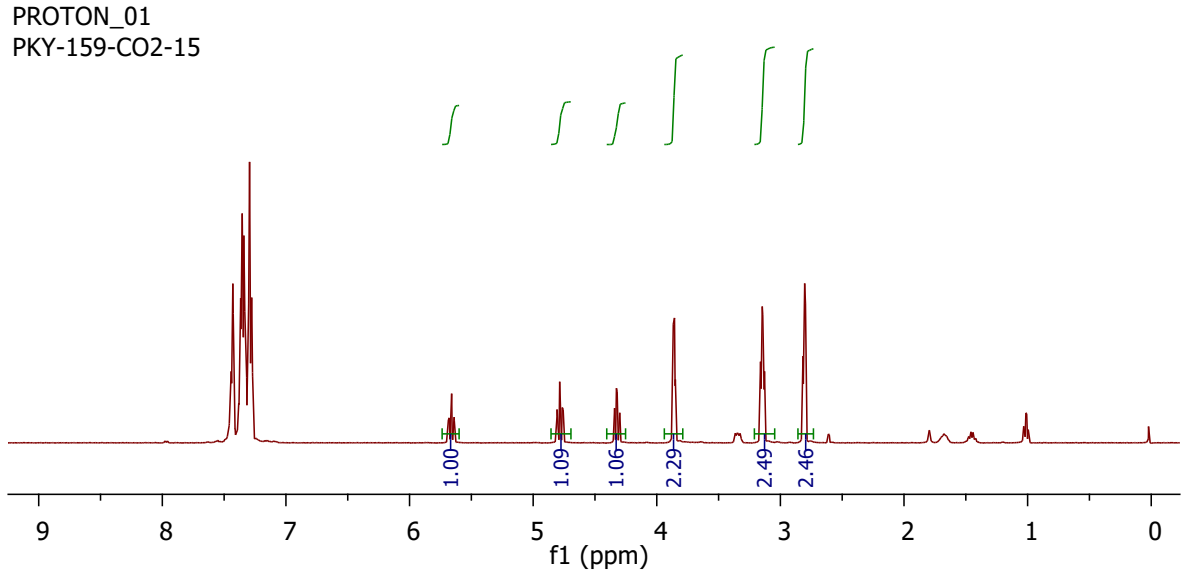

Fig. S14. The Catalytic Reaction Result of Entry 12

(Table 2, Entry 13)

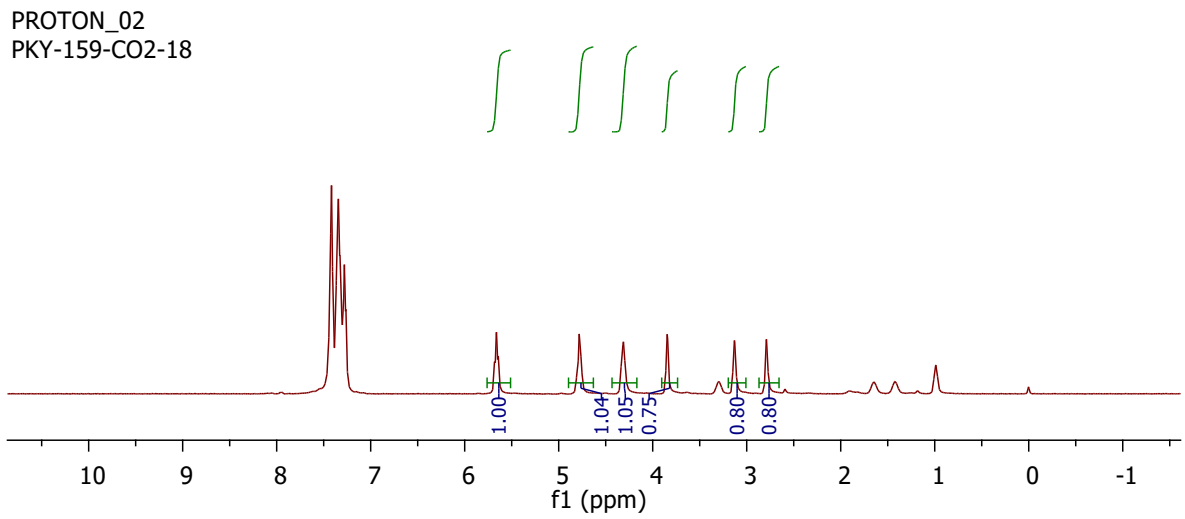

Fig. S15. The Catalytic Reaction Result of Entry 13

Section 5. References

[1] M. Kaya, S. Demir, M. Arıcı, M. Wriedt, O.Z. Yeşilel, Synthesis, characterization, and optical properties of four coordination polymers with 3,5-dicarboxy-1-(4-cyanobenzyl)pyridin-1-ium bromide, Polyhedron. 221 (2022) 115863. https://doi.org/10.1016/J.POLY.2022.115863.

[2] E. Çiftçi, M. Arıcı, E. Demir, R. Demir-Cakan, M. Wriedt, O.Z. Yeşilel, Synthesis, characterization, optical and electrochemical performances of 3-fold interpenetrated Copper(II) coordination polymer with a flexible zwitterionic ligand, J Solid State Chem. 302 (2021) 122375. https://doi.org/10.1016/J.JSSC.2021.122375.